Characterization of fluid-solid phase transition of hard-sphere fluids in cylindrical pore via molecular dynamics simulation

Cite as: J. Chem. Phys. **130**, 164511 (2009); https://doi.org/10.1063/1.3120486
Submitted: 26 November 2008 . Accepted: 27 March 2009 . Published Online: 27 April 2009

Huan Cong Huang, Sang Kyu Kwak, and Jayant K. Singh

Characterization of fluid-solid phase transition of hard-sphere fluids in cylindrical pore via molecular dynamics simulation

Huan Cong Huang,[1] Sang Kyu Kwak,[1,a)] and Jayant K. Singh[2]
[1]*Division of Chemical and Biomolecular Engineering, School of Chemical and Biomedical Engineering, Nanyang Technological University, Singapore 637459, Singapore*
[2]*Department of Chemical Engineering, Indian Institute of Technology Kanpur, Kanpur 208016, India*

(Received 26 November 2008; accepted 27 March 2009; published online 27 April 2009)

Equation of state and structure of hard-sphere fluids confined in a cylindrical hard pore were investigated at the vicinity of fluid-solid transition via molecular dynamics simulation. By constructing artificial closed-packed structures in a cylindrical pore, we explicitly capture the fluid-solid phase transition and coexistence for the pore diameters from 2.17σ to 15σ. There exist some midpore sizes, where the phase coexistence might not exist or not clearly be observable. We found that the axial pressure including coexistence follows oscillatory behavior in different pore sizes; while the pressure tends to decrease toward the bulk value with increasing pore size, the dependence of the varying pressure on the pore size is nonmonotonic due to the substantial change of the alignment of the molecules. The freezing and melting densities corresponding to various pore sizes, which are always found to be lower than those of the bulk system, were accurately obtained with respect to the axial pressure. © *2009 American Institute of Physics*. [DOI: 10.1063/1.3120486]

I. INTRODUCTION

It has been well recognized that confined fluids in nano- to micrometer pore sizes exhibit different properties and behaviors compared to those of bulk fluids at the same thermodynamic conditions.[1–5] An answer to this phenomenon can be found from understanding confining effects toward the structural arrangement and the movement of molecules, which are much restricted than in the bulk.[6,7] In past decades many studies on confinement have been done in typical applications such as porous media, which retain curled and entangled cylindrical pores, and carbon nanotubes (CNTs), which resemble a rigid and straight cylindrical pore. It has been shown that even with a generalized pore shape, the fundamental knowledge of fluid-pore systems can be captured for realistic systems;[8–10] however, the main focus in these systems has been brought into the state of fluids.

In correspondence with the growing demands for understanding solid-phase-related problems in cylindrical confinement, there exist some studies that chose to use the hard cylindrical wall with hard-sphere model out of many candidate models due to its theoretical tractability and repulsive hard-core-oriented nature. The former reason is based on several numerical evidences on the existence of the fluid-solid phase transition in both for bulk[11–14] or confined systems[15] with the absence of attractive interactions. The latter provides the system under effects of dominant influence of entropy, thus leading one to focus on the relation of the phase transition and the structure of confined particles with varying pore sizes. Moreover, this simple model resembles realistic colloidal particles[16–18] and peapod-related system (e.g., C_{60} encapsulated in CNT) that can be described by quasi-one-dimensional approach in statistical mechanics.[19]

Mon and Percus[20] performed *NPT* (i.e., constant number of particles, pressure, and temperature) Monte Carlo (MC) simulation of confined hard-sphere fluid to obtain the effect of narrow pore on the equation of state (i.e., pressure versus density). They found a nonmonotonic change of the equation of state caused from varied structures of confined particles. Later, theoretical quantification for hard-sphere fluids in the very narrow pore was established.[21] In recent years, Gordillo *et al.*[15] observed the onset of freezing shown by a sharp change of the density at certain radii of pores via the same *NPT* MC method and elucidated that the cause of this behavior is microstructural transformation. With effects of the attractive potential, Koga and Tanaka[7] studied Lennard-Jones (LJ) confined fluids analogous to argon atoms trapped in single-wall CNT via molecular dynamics (MD) method. Dependence of temperature and spontaneous structures of soft-sphere particles were examined with respect to variation of phases.

The aforementioned works generally focused on a narrow range of pores, but we wish to extend the idea of pore-size dependence on hard-sphere fluid-solid model with asymptotic increase in pore-size range up to 15σ, where σ is the diameter of the hard sphere, via collision-based MD method. In particular, MD technique enables one to find the accurate fluid-solid coexistence region provided that the configurations are known depending on pore sizes and further to obtain the information of the structural change during the transition. Note that we use the term fluid-solid phase transition or phase transition in place of transition of confined fluids from disordered (i.e., fluidlike) to ordered (i.e., solidlike) state in this paper. The rest of the paper is organized as follows: In Sec. II we briefly introduce the fluid and bound-

a)Author to whom correspondence should be addressed. Electronic mail: skkwak@ntu.edu.sg.

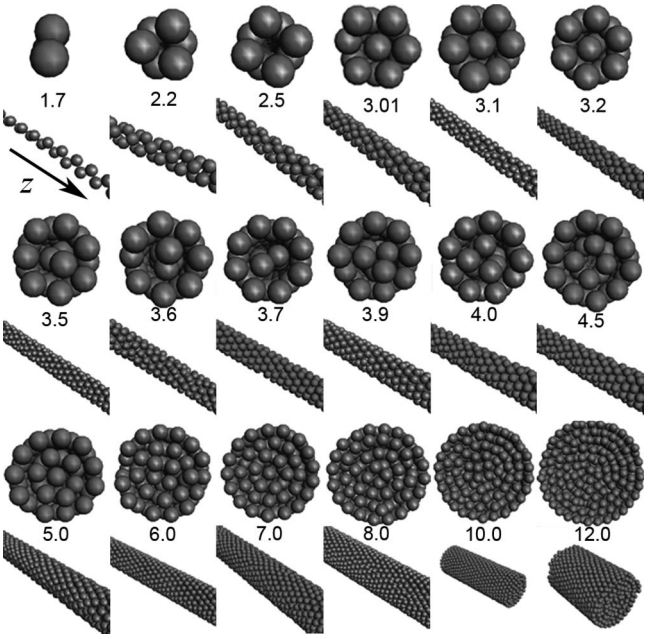

FIG. 1. Screenshots of the simulations at high densities, at which solid structures can be observed. The cross section and side views are shown for different pore sizes for $D=1.7$ (quasi-one-dimensional system), 2.2 and 2.5 (one layer), 3.01, 3.1, 3.2, 3.5, 3.6, 3.7, 3.9, 4.0, and 4.5 (two layers), and 5.0, 6.0, 7.0, 8.0, 10.0, and 12.0 (three or multilayers).

ary model in our simulation and the details of simulation conditions in this work. Section III presents the results and discussion followed by conclusion in Sec. IV.

II. SIMULATION MODEL AND DETAILS

In this work, the fluid-fluid interaction is represented by the hard-sphere potential

$$u_{f\text{-}f}(r_{ij}) = \begin{cases} 0, & r_{ij} \geq \sigma, \\ \infty, & r_{ij} < \sigma, \end{cases} \tag{1}$$

where r_{ij} is the distance between two particles. The cylindrical pore is then modeled by creating an inscribed cylindrical boundary in a rectangular simulation box so that fluid particles are confined in the cylindrical shape. The cylindrical pore is considered perfectly rigid and has no slip, i.e., when a particle collides at the wall, the normal component of its momentum turns into its opposite direction with the same magnitude while the tangential component is invariant. The fluid-wall interaction is represented by the following equation:

$$u_{f\text{-}w}(r) = \begin{cases} 0, & r \geq 0.5\sigma, \\ \infty, & r < 0.5\sigma, \end{cases} \tag{2}$$

where r is the distance from the wall boundary to the center of the particle. Periodic boundary condition is applied along the pore axis, which is set to the z direction (see Fig. 1) in this study.

The units in this work are simulation units, which use amu for mass, Å for length, and ps for time; thus the unit of temperature T^* is amu $Å^2/ps^2$ and that of pressure P^* is amu/Å ps^2. Since we take unity for hard-sphere diameter σ, the number density ρ^* (i.e., $=\rho\sigma^3$) becomes dimensionless. All length scales are in unit of σ. We have performed a series of MD simulations in the microcanonical (*NVE*) ensemble, where N is the number of particles, V is the volume of simulation box, and E is the energy. To construct and perform MD simulations, ETOMICA (Ref. 22) simulation package was employed. The reduced time step Δt^* was set to 0.01. The reduced temperature T^* was fixed at 1.0, as it has no effects to the transition behavior in the hard-sphere system. For the pore diameter less than 4.0σ the simulation was conducted with the system size of 1000 particles, and 2000 or more particles were applied for pores larger than 4.0σ to keep the length of the tube long enough to avoid finite size effects. Simulations of double system size were also conducted to see that there are no significant difference of properties when the length of the tube is long enough. The total time steps for equilibration were set to 10^6 at constant temperature and once the system reached equilibrium, another same number of steps was run in *NVE* ensemble to produce data. Note that we omit σ in the length unit hereafter. For P^*_{zz} (i.e., axial pressure), we use the pressure tensor equation obtained from collision-based virial theorem.[23] Since the system of interest is not under effect of shear stress, we consider only main diagonal terms in the pressure tensor, where P^*_{xx} and P^*_{yy} (e.g., the same magnitude in average) are in the radial direction while P^*_{zz} is in the axial one.

It is generally very difficult to simulate high density systems mainly due to the difficulty of constructing the random and spontaneous systems above the freezing density. The artificially constructed initial packing at high density may affect the properties of the system since these packings are not spontaneously constructed. Those may be at the jammed state that could not be changed to other possible configurations at the same density. A study of spontaneous close-packed structures of hard-sphere particles in cylindrical shape at $T^*=0$ was done by Pickett *et al.*,[6] who found different close-packed configurations of particles in a narrow cylindrical shape (i.e., diameter approximately smaller than 2.2) and the dependence of maximum fraction on pore size. Another study of close-packed structure of confined LJ systems was conducted by Koga and Tanaka.[7] Spontaneous close-packed structure of particles in larger pores becomes severely complex and is still an unsolved problem. To obtain a high density, one solution is starting the simulation at random fluidlike structure and carefully compressing the system to high density using *NPT* MC method. However, by *NPT* scheme, compressing the system from low density to high usually leads a system to a jammed state at high density somewhere above melting or to a metastable state for the worse case. This might have been an issue for Gordillo *et al.*,[15] who did not observe the freezing at $D=2.18$, while we found that at 2.17. Also, their simulations ended at $P^*_{zz}=20.0$, which is lower than the coexistence pressure we found for $D=2.18$. We suspect that they could not perform simulations at higher pressure due to the low probability of volume decrease; the system did not go through chirally ordered solidification. To this end, we realized that *NPT* scheme may not be suitable for accurate determination of the

fluid-solid transition. Thus we develop our own scheme to construct the initial configurations, which can bear the high density enough to be above melting.

Here we give a brief description of this simplified scheme. In the radial direction, the particles are packed into layers of regular polygons with different shapes. Denote the radius of the ith layer within the pore diameter as r_i and the number of sides of a polygon as S_i. We begin with the outer layer. For a pore diameter D, the maximum accessible distance of the center of a particle to the center of the cylinder is $(D-1)/2$; then $r_n=(D-1)/2-\delta$, where n denotes the maximum number of layers and δ is a small number (i.e., 0.001 or smaller), which can be modulated to position the particles radially so that the surface of the particle at the outmost layer does not overlap with the cylindrical wall surface. In the next step, we calculate the maximum possible number of sides S_n of a regular polygon, whose length of side is 1.0 and circumradius is smaller than r_n. Then we lay the center of particles into a regular polygon of S_n side and circumradius r_n. The $(n-1)$th layer is packed with $r_{n-1}=r_n-1.0-\delta$ and the same procedure is repeated until the innermost layer is reached. If the radius of the innermost layer r_1 is not large enough to hold a polygon shape or layer of two atoms, we then pack the particles into a zig-zag structure. In the axial direction, the regular polygons are stacked with the structure $ABAB\cdots$, in which A and B have the same shape, while B rotates with an angle of π/S_i against A. The distance of A and B is set to 0.87 (i.e., slightly larger than $\sqrt{3}/2$ to avoid the overlap of particles and assure enough density). Note that this scheme has some shortcomings; first, it does not produce extremely high density (i.e., near close-packed density in the bulk), and second, at high density, as the packing is not spontaneously constructed, the properties obtained from these initial packing may be specific beyond the melting point. Nevertheless, this compromising solution of packing structure serves our purpose, which predicts the target fluid-solid transition ranges of density and pressure of our interest.

The microscopic structure of the system is monitored by the one-body radial density profile $\rho(r^*)$ and the axial pair distribution function $g(z^*)$, where $r^*=r/\sigma$ and $z^*=z/\sigma$, respectively. For the fluid confined in cylindrical pores, the radial density profile $\rho(r^*)$ is obtained by dividing the pore into n concentric cylindrical shells with the same thickness $\Delta r=(D-1.0)/2n$ then sample the number of particles in each shell divided by the shell volume. Thus, the segment of $\rho(r^*)$ can be expressed as

$$\rho(r_i/\sigma)=\frac{\langle N_i\rangle}{\pi((r_i/\sigma)^2-(r_{i-1}/\sigma)^2)L}, \tag{3}$$

where N_i is the number of particles, whose distances to the pore center are in the range r_{i-1} to r_i, and $r_i=\Delta r\times i$. L is the length of the cylindrical pore. A simple modification from the pair correlation function based on the spherical coordinate can lead to the axial pair distribution function, which is extracted from the following equation:

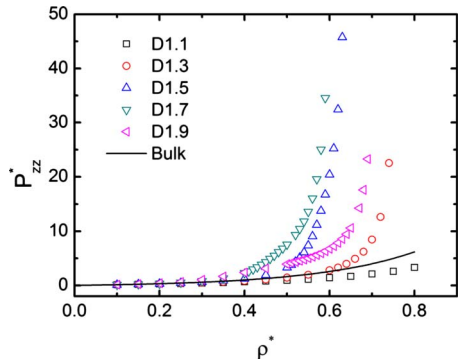

FIG. 2. (Color online) The axial pressure P^*_{zz} vs the average density ρ^* of confined hard spheres in the cylindrical hard pore. The pore diameters are in the range from 1.1 to 1.9. The solid line for Carnahan and Starling's equation of state (Ref. 25) is plotted for comparison. Error is smaller than the size of symbols.

$$\int_{z^*=0}^{z^*=\infty}\rho^* g(z^*)\pi\left(\frac{R}{\sigma}\right)^2 dz^*\approx N, \tag{4}$$

where N is the total number of particles, $\rho=N/V$ is the number density, and R is the radius of the cylindrical pore. The upper limit of Z^* is changed to the axial length of the simulation box, L in calculation. A normalization factor (i.e., $N\rho\pi R^2L$) has been used to present the results in this study.

III. RESULTS AND DISCUSSION

It has been generally considered that a purely one-dimensional system with shot-ranged interactions cannot have a phase transition at finite temperature.[24] Hard-sphere particles confined with pore diameters less than 2.0 can be considered as such kind of system, as each particle can only have two and unchangeable neighbors in interaction and the motions of particles are mostly restricted at one dimension, which is the axis of the cylindrical core (see Fig. 1 for snapshots of confined structures at different pore sizes). Figure 2 presents the equation of state of the aforementioned system. We observe that for $D=1.1$, P^*_{zz} is lower than the bulk value (i.e., Carnahan and Starling[25] and Speedy[26]) at the same density. This is due to less collision of particles, which can be considered as a major confining effect that comes from the presence of narrow pore size; the frequency of occurrence of intercollision between particles is comparable to that of the particle-wall collision. For other pore sizes (i.e., $D=1.3$, 1.5, 1.7, and 1.9), the axial pressures almost overlap with the bulk value at low density, and as density increases, they greatly deviate from the bulk value and diverges to the infinite at the close-packed structures corresponding to their pore sizes. We particularly observe that the dependence of the axial pressure on the pore size is nonmonotonic. Over densities higher than 0.4, it is clear that the axial pressure increases with the pore diameter from 1.1, reaches its maximum around 1.7, and then drops as the diameter increases to 1.9. This behavior indicates the structural change of the confined particles, which can be easily observed by the axial pair distribution function $g(z^*)$ (not shown). We did not observe any discontinuous points indicating the occurrence of the phase transition in these pore sizes.

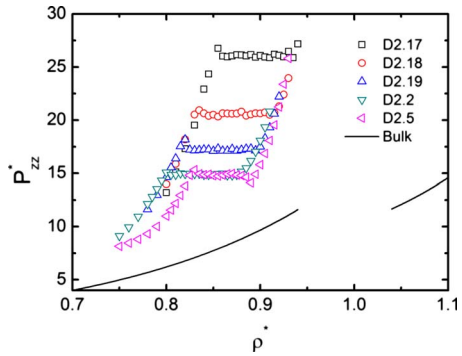

FIG. 3. (Color online) The axial pressure P_{zz}^{*} vs the average density ρ^{*} of confined hard spheres in the cylindrical hard pore. The pore diameters are in the range from 2.17 to 2.5. The solid lines in different phases are obtained from the equation of states for fluids and solids (i.e., face-centered-cubic hard-sphere crystal) from Carnahan and Staring (Ref. 25) and Speedy (Ref. 26), respectively. Error is smaller than the size of symbols.

The axial pressure with respect to the average number density is presented in Fig. 3 for the pore sizes ranged from 2.17 to 2.5. Such systems consist of only one cylindrical layer of particles of twisted helices or simple regular polygon shapes—triangle and square (see Fig. 1). Compared to the case $D \leq 1.9$, these systems show higher packing over unit volume. The axial pressure is always larger than the bulk value over the density of interest; the intercollision between particles is more rigorous than the particle-wall collision. We obtain the smallest pore size (i.e., $D=2.17$) for observing the phase transition of hard-sphere fluids in the hard cylindrical pore. Due to the severe sensitivity of the pore size on the phase transition, we asymptotically increase the diameter to capture the transition of the fluid-solid coexistence region. Note that *NPT* MC method is not easily able to obtain the clear phase transition with the same accuracy. While the pore size gradually increases until 2.2, the axial pressure decreases in a nonmonotonic manner, but the freezing and melting densities linearly decrease with nearly the same range of the coexistence region (i.e., weak dependence on pore size). We observe that the fluidlike (i.e., disordered) structure below the freezing density transforms to the solidlike (i.e., series of triangular polygons in the axial direction)

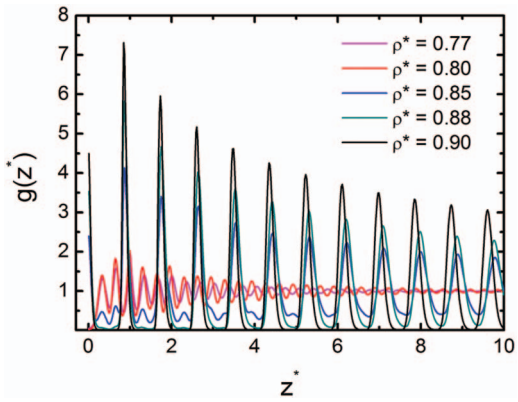

FIG. 4. (Color) The axial distribution function $g(z^{*})$, where $z^{*}=z/\sigma$, at $D=2.2$. The different lines correspond to the densities at fluid branch ($\rho^{*}=0.77$), around freezing density ($\rho^{*}=0.80$), within fluid-solid coexistence ($\rho^{*}=0.85$), around melting density ($\rho^{*}=0.88$), and solid branch ($\rho^{*}=0.90$).

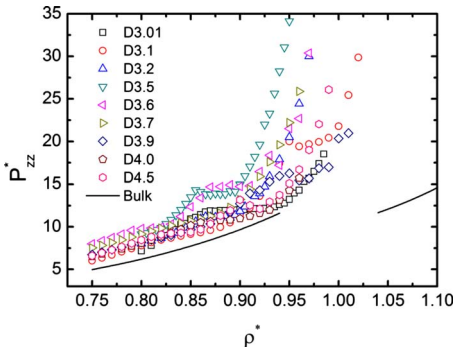

FIG. 5. (Color online) The axial pressure P_{zz}^{*} vs the average density ρ^{*} of confined hard spheres in the cylindrical hard pore. The pore diameters are in the range from 3.01 to 4.5. The solid lines are the same as shown in Fig. 3. Error is smaller than the size of symbols at fluid and solid phases but twice that of the symbols at coexistence.

through forming a twisted helical structure at coexistence. Typical pair distribution functions at $D=2.2$ are presented to show the confined structures at different phase branches in Fig. 4: fluid, around freezing, in coexistence, around melting, and solid branch. Note the appearance of small and irregular shape of peaks among regular peaks at coexistence, which indicates helical shape of the confined particles. Over this range of pore sizes, the confined particles show the same structures except at $D=2.5$. The freezing and melting densities shift to high with a shorter coexistence region but with the same pressure as in $D=2.2$ (i.e., similar intercollision numbers). We attribute this phenomenon to a structural change, in which indeed the tomogram of the confined particles depicts a square (see Fig. 1).

The axial pressures in the systems of two cylindrical layers of particles are presented in Fig. 5. Such systems involve the interactions of particles between different layers, thus making the phase-transition behavior much more complex. Similar to the one layer case, the pressures in these pores are larger than the bulk value at the same density. However, one can expect the oscillatory behavior of the equation of state, which may heavily rely on the confined structure of the particles. Observed in Figs. 1 and 6, the outer-layer particles are aligned following loosely elongated helical shape in the axial direction so that the inner-layer particles form a zigzag (i.e., well fitting of the inner-layer particles onto the contacting surface of the outer-layer par-

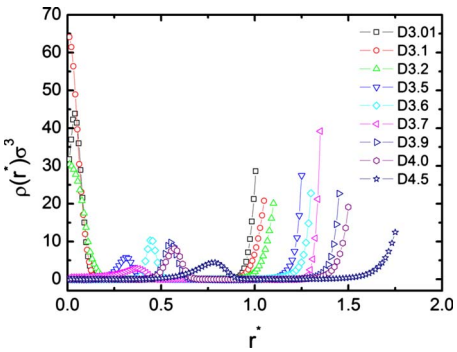

FIG. 6. (Color online) Radial density profiles $\rho(r^{*})\sigma^{3}$, where $r^{*}=r/\sigma$, for the pores in the range from $D=3.01$ to 4.5. The profiles show the different positions formed by the two layers of particles within the pores.

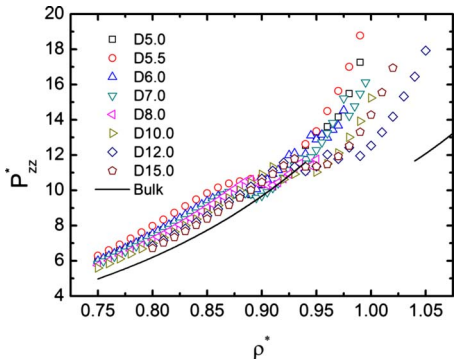

FIG. 7. (Color online) The axial pressure P^*_{zz} vs the average density ρ^* of confined hard spheres in the cylindrical hard pore. The pore diameters are in the range from 5.0 to 15.0. The bulk lines are the same as Figs. 3 and 5. Error is smaller than the size of symbols at fluid and solid phases but twice that of the symbols at coexistence.

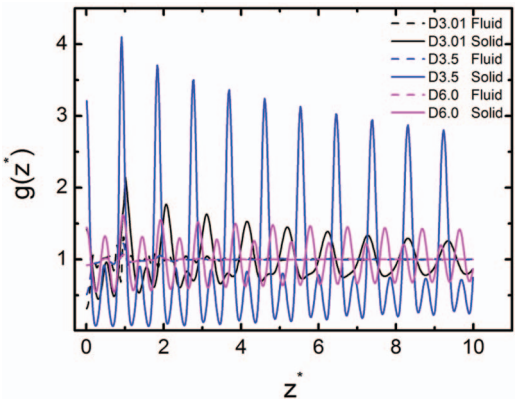

FIG. 8. (Color) The axial pair distribution function $g(z^*)$, where $z^*=z/\sigma$, for the pores $D=3.01$, 3.5, and 6.0 at fluid branch and solid branch, respectively.

ticles) at $D=3.01$, the outer layer is recoiled to form a more compact helical shape, which makes the inner-layer particles aligned in a line at $D=3.1$, and then the hexagonal shape of the outer-layer particles is formed throughout the axial direction with the inner-layer particles formed in a line at $D=3.2$. Indeed, we found the oscillatory values of coexistence pressure and densities. For $D=3.01$, we observed a wide coexistence region (i.e., from $\rho^*\approx 0.870$ to 0.935, indicating a large shift toward the bulk phase-transition region, compared to the case of $D=2.5$) and the coexistence pressure is about 11.9, which is quite close to the coexistence pressure in the bulk. A little increase in the diameter to 3.1 largely shifts the coexistence region (i.e., from $\rho^*\approx 0.950$ to 0.991) and the coexistence pressure is around 20.2, but at $D=3.2$, the coexistence region drops back again (i.e., from $\rho^*\approx 0.863$ to 0.892) with the pressure at around 11.1. While the pore size continuously increases, we found that the system exhibits the oscillatory behavior of the equation of state with the narrow phase-transition region. In particular, over the pore range from 3.5 to 4.5, the largest coexistence pressure was found at $D=3.6$ due to a probable occurrence of the closed-packed structure as similarly found in $D=3.1$. Most interestingly, the phase transition disappears at $D=3.7$. We speculate that the system is the jammed structure, which can be indirectly seen from very low density for the inner layer and high one for the outer layer, which forms a concrete octagon shape. We have also not seen clear phase transitions at $D=3.9$ and 4.0.

For the multilayer systems with three or more layers, the pressure is close to the bulk value of the fluid phase and the phase transition generally happens below the freezing density of the bulk system. The equations of states are presented in Fig. 7 and typical axial pair distribution functions for fluid and solid are presented in Fig. 8 to show the relative structures of the confined particles between small ($D=3.01$ and 3.5) and large ($D=6.0$) pores. Fluid-solid coexistences are clearly observed for $D\geq 6.0$ while those are absent (or not clear) in $D=5.0$ and 5.5. The freezing and melting points shift to higher densities and the coexistence pressure rises as the pore size increases from $D=6.0$ to 8.0. For $D\geq 10$, we found that the coexistence pressure is very close to the bulk value but with a shorter range of the coexisting region. We do not observe a strong oscillatory behavior of the equation of state over this range of the pore sizes indicating less effect of the different packing structures. The values of the freezing and melting densities are presented in Table I with respect to the coexistence axial pressures depending on the pore sizes at the phase transitions. In these large pores, each layer could be regarded as a hexagonal plane rolling into a cylindrical pore in general. As the pore size increases, atoms are less directly affected by the wall boundary so that the bulk structure might be locally formed in the vicinity of the cylinder axis; however, we do not specify a notable threshold to distinguish whether the particles follow the behavior of the bulk system or that of the highly confined one. Lastly, we provide relative axial pressures with respect to those at bulk depending on pore sizes when the density of the system is below 0.7 in Fig. 9. At very low densities from 0.1 to 0.2, the pressures monotonically reduce toward those at bulk as pore sizes increase. As density increases, we observed that the range of pore sizes for the nonmonotonic behavior of the relative

TABLE I. Estimated data of densities at freezing (ρ^*_f) and melting (ρ^*_m) and coexistence axial pressure ($P^*_{zz,\mathrm{coe}}$) for various pore sizes. The coexistence pressure is calculated by averaging the values in the coexistence region. The freezing and melting densities are then estimated by fitting the second-order polynomials to fluid and solid branches, respectively. The values shown in parentheses represent errors in the last digits.

Diameter	ρ^*_f	ρ^*_m	$P^*_{zz,\mathrm{coe}}$
2.17	0.852(1)	0.935(1)	26.1(2)
2.18	0.832(1)	0.914(2)	20.6(1)
2.19	0.813(2)	0.895(4)	17.2(3)
2.2	0.803(1)	0.878(2)	14.91(9)
2.5	0.826(2)	0.893(3)	14.8(4)
3.01	0.870(4)	0.935(3)	11.9(2)
3.1	0.950(1)	0.991(2)	20.2(4)
3.2	0.863(2)	0.892(1)	11.1(1)
3.5	0.852(2)	0.893(2)	13.9(2)
3.6	0.870(1)	0.909(1)	14.8(1)
4.5	0.897(5)	0.929(7)	12.9(6)
6.0	0.858(2)	0.879(6)	9.73(6)
7.0	0.865(3)	0.899(4)	9.8(1)
8.0	0.883(3)	0.911(6)	10.4(1)
10.0	0.903(4)	0.947(8)	11.0(2)
12.0	0.922(1)	0.983(9)	11.7(4)
15.0	0.922(4)	0.961(3)	11.5(1)

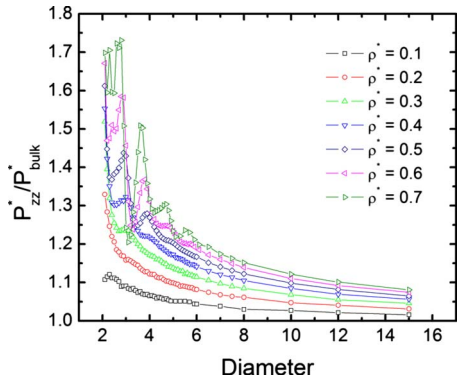

FIG. 9. (Color online) The relative axial pressure (i.e., $P^*_{zz}/P^*_{\mathrm{bulk}}$) vs the diameter of pore for dilute to dense fluids.

pressure becomes larger and the pressures cross over to those at lower densities. This phenomenon indicates that the considerable structural rearrangements started even at liquidlike densities. The nonmonotonic behavior of the relative pressure spreads over larger pore sizes as the density increases; thus complex crossover of the equation of state happens at coexisting and solidlike regions as shown in this work.

IV. CONCLUSION

In this study, we consider cylindrically confined systems under entropic dominance to capture the effects of confinement on the phase transition of disordered particles. In particular, we have determined the equation of state of hard spheres confined in a cylindrical hard pore with a wide range of pore sizes via *NVE* MD method. Besides agreement with others[15,20,21] in that the behaviors of the equation of states highly depend on the pore size when it is narrow, we found that a little variation of the pore diameter dramatically changes the freezing and melting process; large shifts of the freezing and melting densities as well as the coexistence pressure and the degree of property dependence on the pore size become weaker as it increases. We did not observe the phase transition in the pore diameters less than 2 while the transition is observed for the pore diameters larger than 2.16, also suggested by Gordillo *et al.* (i.e., $1+2\sqrt{3}/3$).[15] We presented the detailed data for the coexistence of fluid-solid phase and tracked the structural change during the onset of the fluid-solid transition. Our results predict that all properties found generally do not contain simple monotonic dependences on the pore size mainly due to the diversity of hard-sphere packing structures with respect to different pore sizes. Indeed, certain pore sizes make the systems without any clear phase transitions, but one can consider other spontaneous packing structures, which we leave for a future work.

ACKNOWLEDGMENTS

This work was supported by Nanyang Technological University (Grant Nos. M58120005-SUG and M52120043-RG39/06). Computational resources have been provided by the School of Chemical and Biomedical Engineering.

[1] J. K. Singh and S. K. Kwak, J. Chem. Phys. **126**, 024702 (2007).
[2] K. Koga and H. Tanaka, J. Chem. Phys. **122**, 104711 (2005).
[3] M. C. Gordillo, J. Boronat, and J. Casulleras, Phys. Rev. Lett. **85**, 2348 (2000).
[4] R. Evans, J. Phys.: Condens. Matter **2**, 8989 (1990).
[5] J. Mittal, J. R. Errington, and T. M. Truskett, J. Chem. Phys. **126**, 244708 (2007).
[6] G. T. Pickett, M. Gross, and H. Okuyama, Phys. Rev. Lett. **85**, 3652 (2000).
[7] K. Koga and H. Tanaka, J. Chem. Phys. **124**, 131103 (2006).
[8] C. Huang, K. Nandakumar, P. Y. K. Choi, and L. W. Kostiuk, J. Chem. Phys. **124**, 234701 (2006).
[9] F. R. Hung, G. Dudziak, M. Sliwinska-Bartkowiak, and K. E. Gubbins, Mol. Phys. **102**, 223 (2004).
[10] S. C. Mcgrother and K. E. Gubbins, Mol. Phys. **97**, 955 (1999).
[11] B. J. Alder and T. E. Wainwright, J. Chem. Phys. **27**, 1208 (1957).
[12] W. W. Wood and J. D. Jacobson, J. Chem. Phys. **27**, 1207 (1957).
[13] W. G. Hoover and F. H. Ree, J. Chem. Phys. **49**, 3609 (1968).
[14] H. Reiss and A. D. Hammerich, J. Phys. Chem. **90**, 6252 (1986).
[15] M. C. Gordillo, B. Martinez-Haya, and J. M. Romero-Enrique, J. Chem. Phys. **125**, 144702 (2006).
[16] A. Matsuyama, J. Chem. Phys. **128**, 224907 (2008).
[17] A. J. Banchio and G. Nägele, J. Chem. Phys. **128**, 104903 (2008).
[18] B. S. John, C. Juhlin, and F. A. Escobedo, J. Chem. Phys. **128**, 044909 (2008).
[19] L. A. Girifalco and M. Hodak, Appl. Phys. A: Mater. Sci. Process. **76**, 487 (2003).
[20] K. K. Mon and J. K. Percus, J. Chem. Phys. **112**, 3457 (2000).
[21] I. E. Kamenetskiy, K. K. Mon, and J. K. Percus, J. Chem. Phys. **121**, 7355 (2004).
[22] D. A. Kofke and B. C. Mihalick, Fluid Phase Equilib. **194–197**, 327 (2002).
[23] M. P. Allen and D. J. Tildesley, *Computer Simulation of Liquids* (Clarendon, Oxford, 1987).
[24] L. von Hove, Physica **16**, 137 (1950).
[25] N. F. Carnahan and K. E. Starling, J. Chem. Phys. **51**, 635 (1969).
[26] R. J. Speedy, J. Phys.: Condens. Matter **10**, 4387 (1998).